

Chiral Surface States on the Step Edge in a Weyl Semimetal

Yositake Takane

*Department of Quantum Matter, Graduate School of Advanced Sciences of Matter,
Hiroshima University, Higashihiroshima, Hiroshima 739-8530, Japan*

(Received)

A Weyl semimetal with a pair of Weyl nodes accommodates chiral states on its flat surface if the Weyl nodes are projected onto two different points in the corresponding surface Brillouin zone. These surface states are collectively referred to as a Fermi arc as they appear to connect the projected Weyl nodes. This statement assumes that translational symmetry is present on the surface and hence electron momentum is a conserved quantity. It is unclear how chiral surface states are modified if the translational symmetry is broken by a particular system structure. Here, focusing on a straight step edge of finite width, we numerically analyze how chiral surface states appear on it. It is shown that the chiral surface states are algebraically (i.e., weakly) localized near the step edge. It is also shown that the appearance of chiral surface states is approximately determined by a simple condition characterized by the number of unit atomic layers constituting the step edge together with the location of the Weyl nodes.

1. Introduction

A Weyl semimetal possesses pairs of nondegenerate Dirac cones with opposite chirality.^{1–10)} The band-touching point of each Dirac cone is referred to as a Weyl node. A typical feature of a Weyl semimetal is that low-energy states with chirality appear on its flat surface³⁾ if a pair of Weyl nodes is projected onto two different points in the corresponding surface Brillouin zone. As these surface states appear to connect a pair of projected Weyl nodes, they are collectively called a Fermi arc. The presence of a Fermi arc gives rise to an anomalous Hall effect.⁵⁾ It has been shown experimentally that a Weyl semimetal phase is realized in TaAs and NbAs.^{11–16)}

Usually, the appearance of chiral surface states is argued under the assumption that translational symmetry is present on the surface and hence electron momentum is a conserved quantity. How are chiral surface states modified if the translational symmetry is explicitly broken as a consequence of a particular system structure? Let us focus on a straight step arranged on the flat surface of a Weyl semimetal [see Fig. 1(a)]. On its side surface, which is referred to as a step edge hereafter, the translational symmetry is broken in the perpendicular direction. It has been shown that in a weak topological insulator, surface states on such a step edge exhibit unusual properties.^{17–23)} Let N be the number of unit atomic layers constituting the step edge. If N is very large, the translational symmetry is approximately recovered on the step edge and hence surface states behave in the same way as on an infinitely large flat surface. We thus concentrate on the case where N is relatively small, typically of order ten or smaller.

For definiteness, we focus on the simple system of a Weyl semimetal on a cubic lattice with a pair of Weyl nodes at $\mathbf{k}_{\pm} = (0, 0, \pm k_0)$. On a flat surface parallel to the xy -plane, chiral surface states disappear as \mathbf{k}_{\pm} are projected onto the same point [i.e., $(k_x, k_y) = (0, 0)$] in the corresponding surface Brillouin zone. Contrastingly, chiral surface states appear on a surface parallel to the

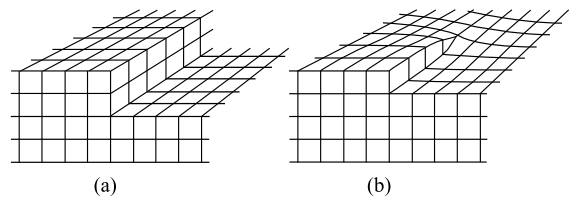


Fig. 1. (a) Straight step edge of $N = 2$. (b) Step edge of $N = 1$ induced by a screw dislocation.

yz - or zx -plane. Let us assume that a straight step consisting of N unit atomic layers is arranged on the flat surface parallel to the xy -plane so that a step edge of height N appears with its surface perpendicular to the xy -plane. Note that this step edge can be related to a screw dislocation along the z -direction with a displacement of N unit atomic layers. If such a screw dislocation is terminated on a flat surface, a step edge of height N originating from the point of termination on the surface inevitably appears [see Fig. 1(b)]. It has been shown that chiral states appear along a screw dislocation in a Weyl semimetal under a certain condition.²⁴⁾ We can expect that if a chiral state is stabilized along the dislocation, it is continuously connected with a chiral surface state on a step edge. Adapting the argument of Ref. 24 to this case, we find that a pair of gapless chiral states is stabilized along a screw dislocation for each odd integer l satisfying $k_0 a > l\pi/N$. Do chiral surface states on a step edge satisfy the same condition? This condition is different from that for chiral surface states in the slab of a Weyl semimetal. If the slab consists of N unit atomic layers stacked in the z -direction, an unpaired chiral surface state appears on its side surface for each positive integer l satisfying $k_0 a > l\pi/(N + 1)$.^{25, 26)}

In this paper, we study the behavior of chiral surface states on a straight step edge of height N in a prototypical Weyl semimetal possessing a pair of Weyl nodes at $\mathbf{k}_{\pm} = (0, 0, \pm k_0)$. We numerically obtain the wave func-

tions of low-energy eigenstates near the Weyl nodes in the model system with two step edges. It is shown that the chiral surface states are algebraically (i.e., weakly) localized near the step edge. This should be contrasted with the strongly localized feature of chiral states on a flat surface or along a screw dislocation. It is also shown that the appearance of chiral surface states is approximately described by a simple condition: an unpaired chiral surface state appears on the step edge for each positive integer j satisfying $k_0 a > j\pi/N$. This condition is different from that for chiral states along a screw dislocation.

In the next section, we present a tight-binding model for a Weyl semimetal and implement it on a lattice system with two step edges. In Sect. 3, we numerically obtain the wave functions of low-energy states near the Weyl nodes. By analyzing the resulting wave functions, we clarify the appearance of chiral surface states on a step edge. The last section is devoted to a summary.

2. Model and Numerical Method

For a Weyl semimetal with a pair of Weyl nodes at $\mathbf{k}_\pm = (0, 0, \pm k_0)$, we introduce a tight-binding model on a cubic lattice with the lattice constant a . The energy at the Weyl nodes is set equal to zero. As our attention is restricted to the system being infinitely long in the x -direction, we hereafter characterize the x dependence of each eigenstate with a wave number k_x . The indices m and n are respectively used to specify lattice sites in the y - and z -directions, and the two-component state vector for the (m, n) th site is expressed as

$$|m, n\rangle = [|m, n\rangle_\uparrow, |m, n\rangle_\downarrow], \quad (1)$$

where \uparrow, \downarrow represents the spin degree of freedom. The tight-binding Hamiltonian is given by $H = H_0 + H_y + H_z$ with^{4,5)}

$$H_0 = \sum_{m,n} |m, n\rangle h_0 \langle m, n|, \quad (2)$$

$$H_y = \sum_{m,n} \{ |m+1, n\rangle h_y^+ \langle m, n| + \text{h.c.} \}, \quad (3)$$

$$H_z = \sum_{m,n} \{ |m, n+1\rangle h_z^+ \langle m, n| + \text{h.c.} \}. \quad (4)$$

Here, the 2×2 matrices are

$$h_0 = \begin{bmatrix} \zeta(k_x) & A \sin(k_x a) \\ A \sin(k_x a) & -\zeta(k_x) \end{bmatrix}, \quad (5)$$

$$h_y^+ = \begin{bmatrix} -B & \frac{1}{2}A \\ -\frac{1}{2}A & B \end{bmatrix}, \quad (6)$$

$$h_z^+ = \begin{bmatrix} -t & 0 \\ 0 & t \end{bmatrix}, \quad (7)$$

with

$$\zeta(k_x) = 2t \cos(k_0 a) + 2B(2 - \cos(k_x a)), \quad (8)$$

where $\pi > k_0 a > 0$, and the other parameters, A , B , and t , are assumed to be real and positive. We find that the energy dispersion of this model is

$$E = \pm \left\{ [\Delta(k_z) + 2B(2 - \cos(k_x a) - \cos(k_y a))]^2 \right.$$

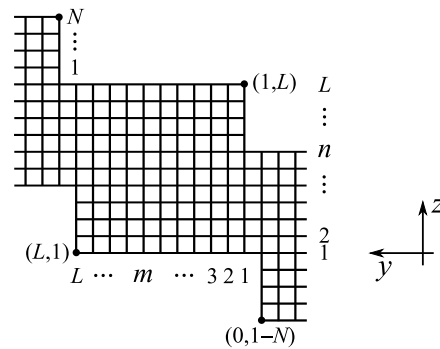


Fig. 2. Cross section of the system considered in the text; it is constructed from a set of $L \times L$ sites by imposing a shifted periodic boundary condition in the y -direction with a shift of N sites. The system is infinitely long in the x -direction and possesses two straight step edges of height N : the lower left step edge includes the corner site at $(L, 1)$ while the upper right one includes that at $(1, L)$. Note that the corner site at $(0, 1-N)$ is identical with that at $(L, 1)$ under the shifted periodic boundary condition.

$$+ A^2 (\sin^2(k_x a) + \sin^2(k_y a)) \Big\}^{\frac{1}{2}} \quad (9)$$

with

$$\Delta(k_z) = -2t [\cos(k_z a) - \cos(k_0 a)]. \quad (10)$$

Equation (9) indicates that a pair of Weyl nodes appears at $\mathbf{k}_\pm = (0, 0, \pm k_0)$, where $E = 0$.

Let us introduce the lattice system with the cross section (see Fig. 2) being constructed from the set of $L \times L$ sites under a shifted periodic boundary condition in the y -direction with the shift of N sites. This is infinitely long in the x -direction and possesses two straight step edges of height N . We apply the tight-binding model given above to this lattice system. As the top and bottom surfaces are parallel to the xy -plane, chiral surface states appear only on the lower left and upper right step edges parallel to the zx -plane. The direction of propagation on one step edge is opposite to that on the other step edge.

As chiral surface states should appear near the Weyl nodes at $E = 0$, we thus numerically obtain the wave functions of eigenstates near zero energy (i.e., low-energy states). We find that the lowest-energy state, as well as lower-energy states in some cases, is algebraically localized near the step edge. That is, a probable chiral surface state is only weakly localized near the step edge. In this situation, we need to examine whether such an algebraically localized state can be a true surface state. Let us suppose that an eigenstate is localized near one step edge when the system size L is large but finite. If its wave function is exponentially (i.e., strongly) localized near the step edge, it is insensitive to the variation of L . Thus, we can definitely judge whether it is a surface localized state. Contrastingly, if its wave function is algebraically (i.e., weakly) localized near the step edge, we must be careful in judging it because a weakly localized state may merge into bulk states with increasing L . In the case of a weakly localized state, the probability density near the step edge monotonically decreases with increasing L . If it converges to a finite value in the large- L limit, the state should be identified as a surface state.

However, the state should be a bulk state if it becomes vanishingly small in the large- L limit. This criterion is rephrased as follows: if the wave function of a weakly localized state is obtained at large but finite L , the state can be identified as a surface state only when the wave function is normalizable even after the extrapolation to the limit of $L \rightarrow \infty$.

We need to deduce the normalizability of a wave function in the large- L limit on the basis of numerical data at large but finite L . To do so, the wave function itself, or its probability distribution, is not convenient as its variation is anisotropic in space. We thus introduce a partially integrated probability distribution $D(i)$ ($i = 1, 2, \dots$) for the two-component wave function $\psi(m, n) = [\psi_\uparrow(m, n), \psi_\downarrow(m, n)]$ of an eigenstate assuming that it is algebraically localized near the lower left step edge including the corner site at $(L, 1)$. Here, $D(i)$ is defined as the summation of the probability density over sites at which the distance from the corner site at $(L, 1)$ is smaller than wi but greater than or equal to $w(i-1)$, where w is an arbitrary length larger than a . That is,

$$D(i) = \sum_{\substack{m, n=1 \\ [wi > R_{m, n} \geq w(i-1)]}}^L (|\psi_\uparrow(m, n)|^2 + |\psi_\downarrow(m, n)|^2), \quad (11)$$

where $R_{m, n}$ denotes the distance between the sites at (m, n) and $(L, 1)$. In determining $R_{m, n}$, the corner site at $(0, 1 - N)$ should be identified as that at $(L, 1)$ under the shifted periodic boundary condition.

From $D(i)$ calculated for a probable chiral surface state at large but finite L , we deduce its fate in the large- L limit. If the decrease in $D(i)$ with increasing i is faster than i^{-1} , the state remains normalizable under the extrapolation to the large- L limit, indicating that it should be identified as a true surface state. Contrastingly, if the decrease in $D(i)$ is slower than i^{-1} , the state is no longer normalizable under the extrapolation to the large- L limit, indicating that it merges into bulk states.

Hereafter, we concentrate on low-energy states with negative energy (i.e., those in the valence band) as they are in one-to-one correspondence with those with positive energy, and set $k_x = 0$ at which the energy of low-energy states becomes closest to zero energy. One may think that the fate of a probable chiral surface state can be judged by observing its energy at $k_x = 0$ as it should vanish in the large- L limit. However, this is prevented by a finite-size gap due to the coupling of chiral surface states weakly localized near the two different step edges. As low-energy states are not degenerate, we simply number them in the valence band from top to bottom such that the highest and next-highest eigenstates are respectively called the first and second states. The first state corresponds to the lowest-energy state closest to zero energy. Preliminary numerical results suggest that an unpaired chiral surface state appears whenever $k_0 a$ exceeds $l\pi/N$ for each positive integer l . Clearly, this condition is different from that for chiral states along the corresponding screw dislocation. We thus adopt the working

hypothesis that the j th state becomes a chiral surface state when $k_0 a > j\pi/N$. For later convenience, we define \tilde{k}_0 as

$$\tilde{k}_0 \equiv \frac{k_0 a}{\pi}, \quad (12)$$

in terms of which the condition of $k_0 a > j\pi/N$ is rewritten as $\tilde{k}_0 > j/N$.

3. Numerical Analysis

We present the numerical results of $D(i)$ for low-energy states to examine the working hypothesis for the appearance of chiral surface states on a step edge. The states with odd j and those with even j are separately analyzed because finite-size effects are weaker in the former than in the latter. We treat the system of $L = 1400$ with step heights of $N = 1, 2, 3, 4$, and 10 . The parameters are set equal to $B/A = t/A = 0.5$ and $w/a = 4$ with $k_x = 0$.

We first consider the case of $N = 1$, in which the hypothesis suggests that no chiral surface state appears. Indeed, although the hypothesis superficially indicates that a chiral surface state appears if $\tilde{k}_0 > 1$, this is never satisfied as \tilde{k}_0 is restricted to be smaller than one. To examine the absence of a chiral surface state, we analyze the behavior of $D(i)$ for the first state at $\tilde{k}_0 = 0.85, 0.90, 0.93$, and 0.96 . The numerical results are shown in Fig. 3(a), where solid lines designate the i^{-1} dependence. We observe that the decrease in $D(i)$ becomes faster with increasing \tilde{k}_0 and that its i dependence asymptotically approaches i^{-1} with increasing \tilde{k}_0 . That is, the decrease in $D(i)$ does not become faster than i^{-1} . This implies that a chiral surface state does not appear in the case of $N = 1$,²⁷⁾ which is consistent with the hypothesis.

We next consider the cases of $N = 2$ and 3 . In these cases, the hypothesis suggests that the first state, which should be a bulk state when $\tilde{k}_0 < 1/N$, becomes a chiral surface state when $\tilde{k}_0 > 1/N$. To examine this, we calculate $D(i)$ for this state at $k_0 = 1/N + \delta\tilde{k}_0$ with deviations of $\delta\tilde{k}_0 = 0, \pm 0.02$, and ± 0.05 . Figures 3(b) and 3(c) respectively show $D(i)$ in the cases of $N = 2$ and 3 , where solid lines designate the i^{-1} dependence. We observe that in both cases, $D(i)$ at $\delta\tilde{k}_0 = 0$ approximately satisfies i^{-1} in the region of $i > 10$ and that the decrease in $D(i)$ becomes faster with increasing $\delta\tilde{k}_0$. That is, the decrease in $D(i)$ becomes faster than i^{-1} when $\delta\tilde{k}_0 > 0$. This result supports the hypothesis that the first state becomes a chiral surface state under the condition of $\tilde{k}_0 > 1/N$. The second state in the case of $N = 3$ is considered later.

We turn to the case of $N = 4$ with focus on the states with odd j , for which the hypothesis suggests that the first state becomes a surface state once \tilde{k}_0 exceeds $1/4$ and then the third state becomes another surface state when \tilde{k}_0 exceeds $3/4$. We thus calculate $D(i)$ for the first state at $\tilde{k}_0 = 1/4 + \delta\tilde{k}_0$ and that for the third state at $\tilde{k}_0 = 3/4 + \delta\tilde{k}_0$ with $\delta\tilde{k}_0 = 0, \pm 0.02$, and ± 0.05 . Figures 4(a) and 4(b) respectively show $D(i)$ for the first state with \tilde{k}_0 close to $1/4$ and that for the third state with \tilde{k}_0 close to $3/4$, where solid lines designate the i^{-1} dependence. We observe that in both cases, $D(i)$ at $\delta\tilde{k}_0 = 0$ approximately satisfies i^{-1} in the region of $i > 10$ and

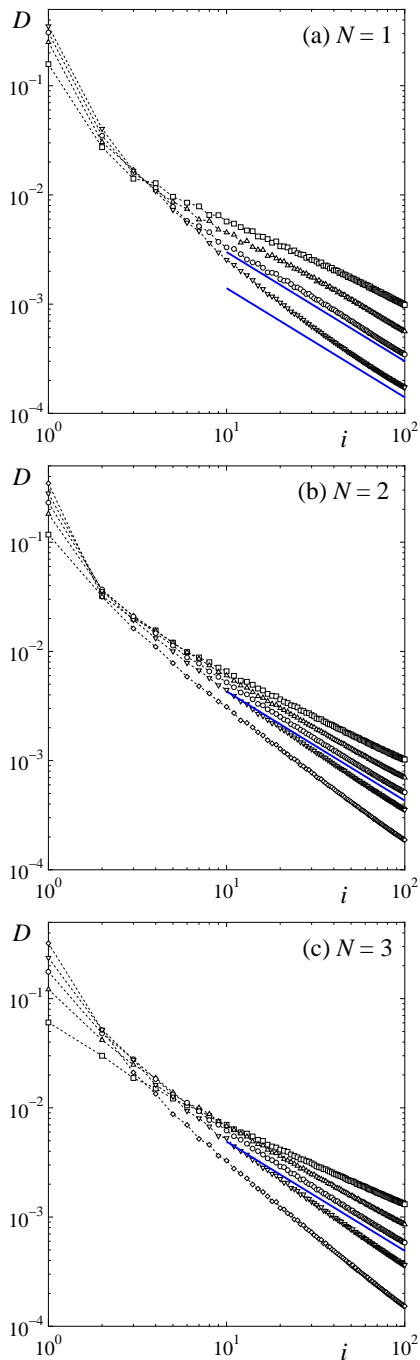


Fig. 3. (Color online) D for the first state as functions of i in the cases of (a) $N = 1$, (b) $N = 2$, and (c) $N = 3$. In the case of (a) $N = 1$, squares, triangles, circles, and down-pointing triangles respectively represent $\tilde{k}_0 = 0.85, 0.90, 0.93$, and 0.96 . In both the cases of (b) $N = 2$ with $\tilde{k}_0 = 1/2 + \delta\tilde{k}_0$ and (c) $N = 3$ with $\tilde{k}_0 = 1/3 + \delta\tilde{k}_0$, squares, triangles, circles, down-pointing triangles, and diamonds respectively represent $\delta\tilde{k}_0 = -0.05, -0.02, 0, 0.02$, and 0.05 . Solid lines designate the i^{-1} dependence.

that the decrease in $D(i)$ becomes faster with increasing $\delta\tilde{k}_0$. That is, the decrease in $D(i)$ becomes faster than i^{-1} when $\delta\tilde{k}_0 > 0$. This result again supports the hypothesis.

Let us consider the second state in the cases of $N = 4$ as well as $N = 3$. Figure 5(a) shows $D(i)$ for this state in the case of $N = 4$ at $\tilde{k}_0 = 2/4 + \delta\tilde{k}_0$ with $\delta\tilde{k}_0 = -0.02, 0, 0.02$, and 0.05 , where the solid line designates the i^{-1} dependence. Remember that the third state becomes a

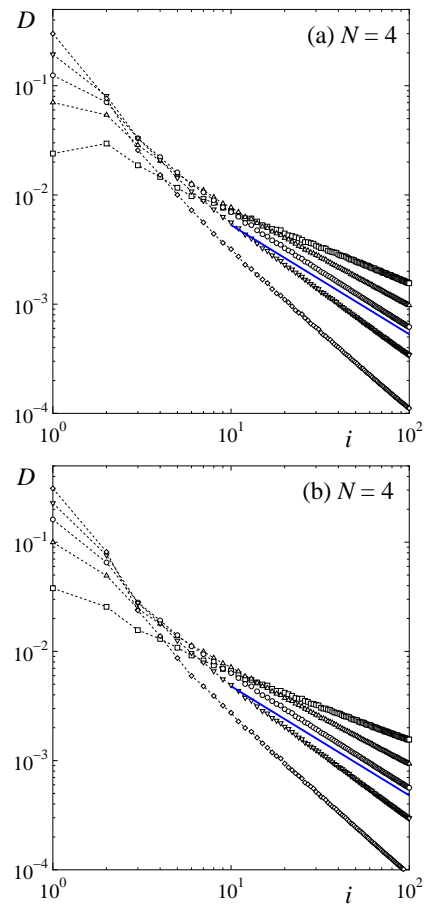


Fig. 4. (Color online) D for the (a) first and (b) third states as functions of i in the case of $N = 4$. In both (a) the first-state case with $\tilde{k}_0 = 1/4 + \delta\tilde{k}_0$ and (b) the third-state case with $\tilde{k}_0 = 3/4 + \delta\tilde{k}_0$, squares, triangles, circles, down-pointing triangles, and diamonds respectively represent $\delta\tilde{k}_0 = -0.05, -0.02, 0, 0.02$, and 0.05 .

chiral surface state when $\tilde{k}_0 > 3/4$, with the consequence that its energy vanishes in the large- L limit. This indicates that, at least under the condition of $\tilde{k}_0 > 3/4$, the second state should be identified as a chiral surface state as its energy is smaller than that of the third state. Hence, the second state must become a chiral surface state at some point within the interval of $3/4 > \tilde{k}_0 > 1/4$. Although $D(i)$ deviates from power-law behavior as i approaches 10^2 , this should be attributed to finite-size effects in accordance with the argument given above. From Fig. 5(a), we observe that the decrease in $D(i)$ becomes faster than i^{-1} when $\delta\tilde{k}_0 \gtrsim 0$. This indicates that the second state becomes a chiral surface state near $\tilde{k}_0 = 2/4$. Here, we turn to the second state in the case of $N = 3$. Figure 5(b) shows $D(i)$ for this state at $\tilde{k}_0 = 2/3 + \delta\tilde{k}_0$ with $\delta\tilde{k}_0 = -0.02, 0, 0.02, 0.05$, and 0.08 , where the solid line designates the i^{-1} dependence. As $D(i)$ significantly deviates from power-law behavior as i approaches 10^2 , it is not easy to obtain a definite conclusion from Fig. 5(b). However, if this deviation can also be attributed to finite-size effects as in the case of $N = 4$, we observe that the decrease in $D(i)$ becomes faster than i^{-1} when $\delta\tilde{k}_0 \gtrsim 0$. This indicates that the second state becomes a chiral surface state near $\tilde{k}_0 = 2/3$. The results

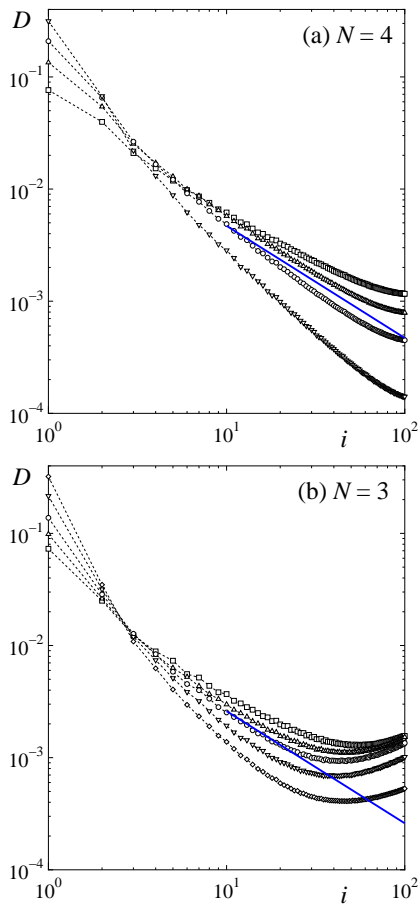


Fig. 5. (Color online) D for the second state as functions of i in the cases of (a) $N = 4$ and (b) $N = 3$. In the case of (a) $N = 4$ with $\tilde{k}_0 = 2/4 + \delta\tilde{k}_0$, squares, triangles, circles, and down-pointing triangles respectively represent $\delta\tilde{k}_0 = -0.02, 0, 0.02,$ and 0.05 . In the case of (b) $N = 3$ with $\tilde{k}_0 = 2/3 + \delta\tilde{k}_0$, squares, triangles, circles, down-pointing triangles, and diamonds respectively represent $\delta\tilde{k}_0 = -0.02, 0, 0.02, 0.05,$ and 0.08 .

obtained above again support the hypothesis. As is also shown in Fig. 6(c), finite-size effects are stronger in the states with even j than in those with odd j . The reason for this is unclear at present.

Finally, we consider the case of $N = 10$ with focus on the states with odd j , for which the hypothesis suggests that the first, third, fifth, seventh, and ninth states respectively become a chiral surface state when \tilde{k}_0 exceeds $1/10, 3/10, 5/10, 7/10,$ and $9/10$. To examine this, we analyze the behavior of $D(i)$ for the first state with \tilde{k}_0 close to $1/10$ and that for the fifth state with \tilde{k}_0 close to $5/10$. Figure 6(a) shows $D(i)$ for the first state at $\tilde{k}_0 = 1/10 + \delta\tilde{k}_0$ with $\delta\tilde{k}_0 = -0.05, -0.02, -0.01, 0,$ and 0.02 , where the solid line designates the i^{-1} dependence. We observe that $D(i)$ approximately satisfies i^{-1} at $\delta\tilde{k}_0 = -0.01$ and decreases faster than i^{-1} at $\delta\tilde{k}_0 = 0$. This implies that the first state becomes a chiral surface state even when \tilde{k}_0 is close to but smaller than $1/10$, slightly inconsistent with the hypothesis. However, as the quantitative deviation from the hypothesis is small, we can say that the hypothesis approximately holds in this case. Although not shown here, behavior similar to this is also seen in $D(i)$ for the ninth state with \tilde{k}_0 close to

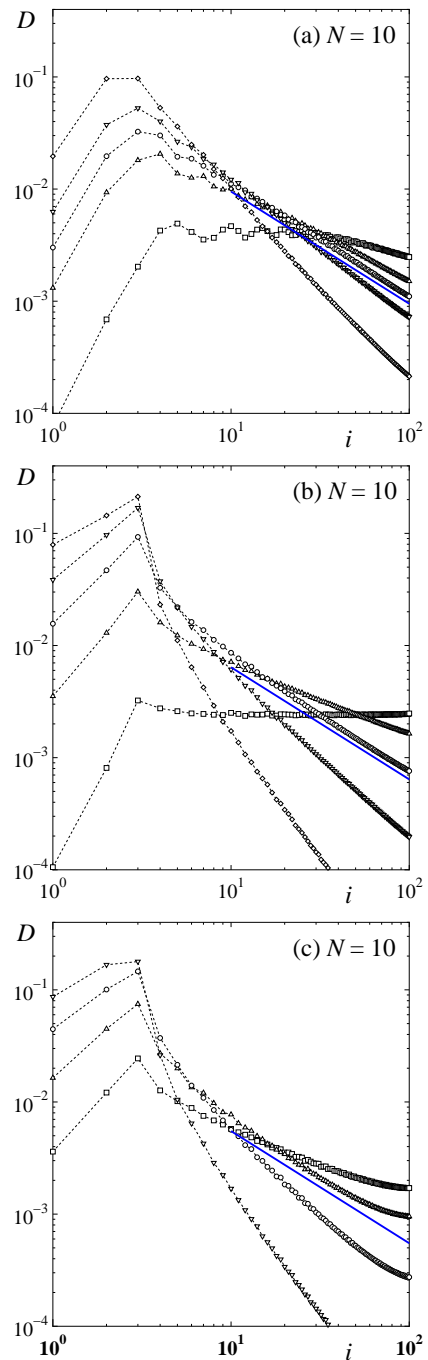


Fig. 6. (Color online) D for the (a) first, (b) fifth, and (c) sixth states as functions of i in the case of $N = 10$. In (a) the first-state case with $\tilde{k}_0 = 1/10 + \delta\tilde{k}_0$, squares, triangles, circles, down-pointing triangles, and diamonds respectively represent $\delta\tilde{k}_0 = -0.05, -0.02, -0.01, 0,$ and 0.02 . In (b) the fifth-state case with $\tilde{k}_0 = 5/10 + \delta\tilde{k}_0$, squares, triangles, circles, down-pointing triangles, and diamonds respectively represent $\delta\tilde{k}_0 = -0.05, -0.02, 0, 0.02,$ and 0.05 . In (c) the sixth-state case with $\tilde{k}_0 = 6/10 + \delta\tilde{k}_0$, squares, triangles, circles, and down-pointing triangles respectively represent $\delta\tilde{k}_0 = -0.02, 0, 0.02,$ and 0.05 .

$9/10$. The slight inconsistency observed in the first and ninth states may suggest that the hypothesis holds in a precise manner only when N is sufficiently small. Figure 6(b) shows $D(i)$ for the fifth state at $\tilde{k}_0 = 5/10 + \delta\tilde{k}_0$ with $\delta\tilde{k}_0 = -0.05, -0.02, 0, 0.02,$ and 0.05 , where the solid line designates the i^{-1} dependence. The decrease

in $D(i)$ becomes faster than i^{-1} when $\delta\tilde{k}_0 > 0$. This result supports the hypothesis. Although not shown here, behavior similar to this is also seen in $D(i)$ for the third state with \tilde{k}_0 close to $3/10$ and for the seventh state with \tilde{k}_0 close to $7/10$.

Here, let us consider the states with even j in the case of $N = 10$. Figure 6(c) shows $D(i)$ for the sixth state at $\tilde{k}_0 = 6/10 + \delta\tilde{k}_0$ with $\delta\tilde{k}_0 = -0.02, 0, 0.02,$ and 0.05 , where the solid line designates the i^{-1} dependence. Although $D(i)$ deviates from power-law behavior as i approaches 10^2 owing to finite-size effects, we observe that the decrease in $D(i)$ becomes faster than i^{-1} when $\delta\tilde{k}_0 \gtrsim 0$. This indicates that the sixth state becomes a chiral surface state near $\tilde{k}_0 = 6/10$. Numerical results for the second, fourth, and eighth states (not shown here) also indicate that they respectively become a chiral surface state near $\tilde{k}_0 = 2/10, 4/10,$ and $8/10$. These results again support the hypothesis.

4. Summary

We numerically studied the behavior of chiral surface states on a straight step edge with N unit atomic layers arranged on the flat surface of a Weyl semimetal possessing a pair of Weyl nodes at $\mathbf{k}_\pm = (0, 0, \pm k_0)$. We showed that they are algebraically localized near the step edge. We also showed that the appearance of chiral surface states is approximately determined by a simple condition characterized by N and k_0 : an unpaired chiral surface state appears for each positive integer j when $k_0 a$ exceeds $j\pi/N$, where a is the lattice constant. Remember that this condition describes the appearance in the limit of the system size L going to infinity. If L is large but finite, a weakly localized surface state may appear even though the condition is not satisfied. Without satisfying it, however, the probability density near the step edge monotonically decreases to zero with increasing L . In other words, the condition ensures the persistence of a chiral surface state in the large- L limit.

Our analysis of chiral surface states is restricted to the case where the transverse wave number k_x is zero. How do they change if k_x deviates from zero? A chiral surface state at $k_x = 0$ likely merges into bulk states with increasing or decreasing k_x in a gradual manner. If the condition of $k_0 a > j\pi/N$ is critically satisfied for a given j , we expect that the corresponding chiral surface state at $k_x = 0$ will be fragile against an increase or decrease in k_x . That is, it will rapidly merge into bulk states with increasing or decreasing k_x . In contrast, if the condition is sufficiently satisfied so that $k_0 a \gg j\pi/N$, the chiral surface state at $k_x = 0$ will be robust against an increase or decrease in k_x .

Acknowledgment

This work was supported by JSPS KAKENHI Grant Number 15K05130.

- 1) G. E. Volovik, *The Universe in a Helium Droplet* (Oxford University Press, Oxford, 2003).
- 2) S. Murakami, *New J. Phys.* **9**, 356 (2007).
- 3) X. Wan, A. M. Turner, A. Vishwanath, and S. Y. Savrasov, *Phys. Rev. B* **83**, 205101 (2011).
- 4) K.-Y. Yang, Y.-M. Lu, and Y. Ran, *Phys. Rev. B* **84**, 075129 (2011).
- 5) A. A. Burkov and L. Balents, *Phys. Rev. Lett.* **107**, 127205 (2011).
- 6) A. A. Burkov, M. D. Hook, and L. Balents, *Phys. Rev. B* **84**, 235126 (2011).
- 7) W. Witczak-Krempa and Y. B. Kim, *Phys. Rev. B* **85**, 045124 (2012).
- 8) P. Delplace, J. Li, and D. Carpentier, *Europhys. Lett.* **97**, 67004 (2012).
- 9) G. Halász and L. Balents, *Phys. Rev. B* **85**, 035103 (2012).
- 10) A. Sekine and K. Nomura, *J. Phys. Soc. Jpn.* **82**, 033702 (2013).
- 11) H. Weng, C. Fang, Z. Fang, B. A. Bernevig, and X. Dai, *Phys. Rev. X* **5**, 011029 (2015).
- 12) S.-M. Huang, S.-Y. Xu, I. Belopolski, C.-C. Lee, G. Chang, B. Wang, N. Alidoust, G. Bian, M. Neupane, C. Zhang, S. Jia, A. Bansil, H. Lin, and M. Z. Hasan, *Nat. Commun.* **6**, 7373 (2015).
- 13) S.-Y. Xu, I. Belopolski, N. Alidoust, M. Neupane, G. Bian, C. Zhang, R. Sankar, G. Chang, Z. Yuan, C.-C. Lee, S.-M. Huang, H. Zheng, J. Ma, D. S. Sanchez, B. Wang, A. Bansil, F. Chou, P. P. Shibayev, H. Lin, S. Jia, and M. Z. Hasan, *Science* **349**, 613 (2015).
- 14) B.-Q. Lv, H.-M. Weng, B.-B. Fu, X.-P. Wang, H. Miao, J. Ma, P. Richard, X.-C. Huang, L.-X. Zhao, G.-F. Chen, Z. Fang, X. Dai, T. Qian, and H. Ding, *Phys. Rev. X* **5**, 031013 (2015).
- 15) B. Q. Lv, N. Xu, H. M. Weng, J. Z. Ma, P. Richard, X. C. Huang, L. X. Zhao, G. F. Chen, C. E. Matt, F. Bisti, V. N. Strocov, J. Mesot, Z. Fang, X. Dai, T. Qian, M. Shi, and H. Ding, *Nat. Phys.* **11**, 724 (2015).
- 16) S.-Y. Xu, N. Alidoust, I. Belopolski, Z. Yuan, G. Bian, T.-R. Chang, H. Zheng, V. N. Strocov, D. S. Sanchez, G. Chang, C. Zhang, D. Mou, Y. Wu, L. Huang, C.-C. Lee, S.-M. Huang, B. Wang, A. Bansil, H.-T. Jeng, T. Neupert, A. Kaminski, H. Lin, S. Jia, and M. Z. Hasan, *Nat. Phys.* **11**, 748 (2015).
- 17) Y. Yoshimura, A. Matsumoto, Y. Takane, and K.-I. Imura, *Phys. Rev. B* **88**, 045408 (2013).
- 18) T. Arita and Y. Takane, *J. Phys. Soc. Jpn.* **83**, 124716 (2014).
- 19) C. Pauly, B. Rasche, K. Koepf, M. Liebmann, M. Pratzner, M. Richter, J. Kellner, M. Eschbach, B. Kaufmann, L. Plucinski, C. M. Schneider, M. Ruck, J. van den Brink, and M. Morgenstern, *Nat. Phys.* **11**, 338 (2015).
- 20) A. Matsumoto, T. Arita, Y. Takane, Y. Yoshimura, and K.-I. Imura, *Phys. Rev. B* **92**, 195424 (2015).
- 21) J.-J. Zhou, W. Feng, G.-B. Liu, and Y. Yao, *New J. Phys.* **17**, 015004 (2015).
- 22) T. Arita and Y. Takane, *J. Phys. Soc. Jpn.* **85**, 033706 (2016).
- 23) C. Pauly, B. Rasche, K. Koepf, M. Richter, S. Borisenko, M. Liebmann, M. Ruck, J. van den Brink, and M. Morgenstern, *ACS Nano* **10**, 3995 (2016).
- 24) K.-I. Imura and Y. Takane, *Phys. Rev. B* **84**, 245415 (2011).
- 25) Y. Takane, *J. Phys. Soc. Jpn.* **85**, 124711 (2016).
- 26) Y. Yoshimura, W. Onishi, K. Kobayashi, T. Ohtsuki, and K.-I. Imura, *Phys. Rev. B* **94**, 235414 (2016).
- 27) An accurate numerical solution is not obtained within the interval of $0.995 > \tilde{k}_0 > 0.96$, possibly owing to the interference between the almost degenerate first states in the valence and conduction bands. Hence, this conclusion is tentative in a strict sense.